

C-scan and L-scan generated images of the concrete/GFRP composite interface

T. Kundu^{a,*}, M. Ehsani^a, K.I. Maslov^b, D. Guo^a

^a*Department of Civil Engineering and Engineering Mechanics, University of Arizona, Tucson, AZ 85721, USA*

^b*Semenov Institute of Chemical Physics, Russian Academy of Science, Moscow 117334, Russia*

Received 10 January 1998; received in revised form 4 June 1998; accepted 8 June 1998

Abstract

Glass Fiber Reinforced Plastics (GFRP) are fast becoming a viable new construction material. They are being used for rehabilitating old concrete structures—columns, beams, slabs and walls—by gluing the composite plate to the concrete surface. Proper attachment between the GFRP plate and the concrete surface is necessary for efficient use of GFRP composites to increase the strength of the rehabilitated structures. Delamination between the rehabilitated structure and the GFRP plate significantly reduces the strength of the reinforced structure. Hence, delamination defects, if present at the interface, should be detected as soon as possible. In this paper, two ultrasonic techniques to detect delamination defects between the GFRP plate and the concrete surface are presented. One technique uses longitudinal waves or P-waves and the second technique uses Lamb waves. It is found that both techniques can detect the defect when used properly. However, Lamb waves give a better image quality of the defect than longitudinal waves. © 1998 Elsevier Science Ltd. All rights reserved.

1. Introduction:

In recent years, significant attention has been paid to the nation's dilapidated infrastructure. Examples of such structures include buildings that need to be retrofitted to resist seismic loads, bridges that must be strengthened to carry heavier traffic loads and concrete water and sewer pipes that have deteriorated due to corrosion. In most of these cases, the capacity of these structures can be increased by the introduction of additional tension-carrying materials. While steel has been traditionally used for such applications, fiber reinforced plastic (FRP) materials have been increasingly replacing steel over the last decade. The high tensile strength and corrosion resistance of FRPs make them an ideal substitute for steel.

FRP plates can be epoxy bonded to the tension face of concrete beams, for example, to increase the flexural capacity of these members significantly [1]. Masonry and concrete walls can be similarly strengthened and there are reported field applications of these techniques to buildings damaged in recent earthquakes [2, 3]. The success of such construction depends in large part on the bond between the FRP plates and the concrete substrate. Thus, there is a great need for development of nondestructive testing methods that could easily identify defects in the bond line.

Ultrasonic techniques have become one of the most popular nondestructive testing techniques because of their versatility and ease of operation. They can easily detect internal cracks and inclusion-type defects in homogeneous or layered materials. However, they have their own shortcomings. They cannot penetrate very deep inside a highly attenuative material. Fibers in the FRP plate scatter away the ultrasonic energy and the epoxy resins used for the matrix material are very attenuative. Hence, these materials are difficult to inspect by ultrasonic signals if the transducers are used in the conventional frequency range (1–10 MHz). Only relatively low frequency ultrasonic waves can propagate through these materials.

In this research, relatively low frequency (below 1 MHz) transducers are used to inspect the delamination between the concrete and the composite plate. Both longitudinal and Lamb waves are generated and used in this investigation. Although the use of longitudinal or P-waves for detecting internal defects in a material is not new, it is new for this particular application, i.e. for detecting delamination between concrete and FRP plates. A Lamb wave imaging technique or L-scan ('L' stands for Lamb) technique is comparatively new. Previous efforts at using Lamb waves to inspect defects in composite and metal plates include the works of Chimenti and Nayfeh [4], Nagy et al. [5], Nayfeh [6], Bar-Cohen and Chimenti [7], Chimenti and Bar-Cohen [8], Martin and Chimenti [9], Mal and Bar-Cohen [10],

* Corresponding author.

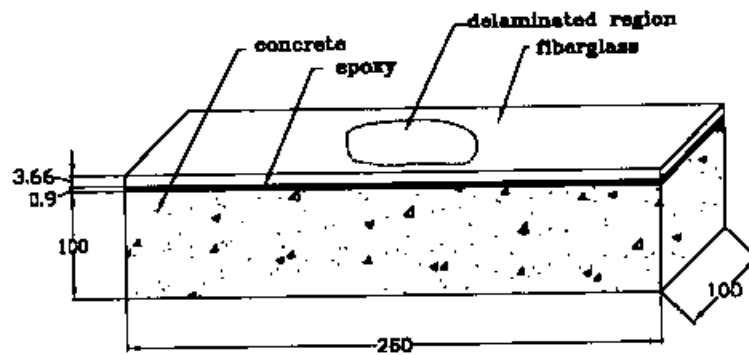


Fig. 1. Geometry of the specimen—epoxy bonded concrete–GFRP plate.

Tang and Henneke [11], Bridge and Ramli [12], Atalar et al. [13, 14], Chimenti and Martin [15], Alleyne and Cowley [16], Rose et al. [17], Pilarski and Rose [18], Challis and Bork [19], Tung et al. [20], Corouble et al. [21], Ditri and Rose [22], among others. Most of these works involve relating the material defects such as porosity and delamination to the change in the Lamb wave propagation characteristics, the dispersion curves, phase velocity and attenuation.

Only a few investigators have so far attempted to scan a specimen using Lamb waves to detect defects inside a material. Chimenti and Martin [15] attempted it and were successful to some extent in detecting internal defects in a composite plate. The major problem of their technique is that it is very sensitive to the plate thickness variation. Hence, a small percentage change in the plate thickness alters the receiver voltage amplitude significantly. To avoid this problem one needs to filter the received signal peak amplitude data through a special filter, called the MFq filter [15]. This signal processing helps to minimize the effect of the plate thickness variation on the null zone but apparently retains the sensitivity of the reflected signal to the internal defects.

Kundu et al. [23] have shown that the problem imposed by the slight variation in the plate thickness can be avoided by placing the receiver beyond the null-zone so that only propagating leaky Lamb waves can be received by the receiver. The wave amplitude in this region is comparatively less sensitive to the plate thickness variation and more sensitive to the defects inside the plate. Kundu and his coworkers have used this transmitter–receiver arrangement for studying composites and interfaces [24–27]. A similar arrangement is used in this study as well.

2. Experiment

2.1. Specimen preparation

A specimen containing a hidden artificial defect is fabricated and scanned by different ultrasonic waves to see under what conditions the delamination defect can be detected clearly. A small interface defect in a real structure

can act as the initiation point for a large area of delamination and can significantly reduce the load carrying capacity of the structure. That is why it is necessary to detect defects when they are small (a few centimeters in dimension for civil engineering structures). The specimen was prepared by gluing a glass fiber reinforced plastic (GFRP) plate to a concrete block as shown in Fig. 1. The GFRP plate was manufactured by pressing three layers of an E-glass fabric in a polyester resin matrix. The fabric weighed approximately 18 oz per square yard (0.61 kg m^{-2}) and had equal amounts of fibers in the 0 and 90° directions. The average thickness of the plate was 3.66 mm. A two-component epoxy was mixed to produce an adhesive with a consistency of warm honey. The epoxy was applied to the surface of the GFRP plate before it was placed on top of the concrete block. A small pressure [less than 1 psi (6890 Pa)] was applied to the GFRP plate at room temperature for about 2 days until the epoxy was cured. The average total thickness of glue and GFRP plate was found to be 4.56 mm. While preparing the specimen an approximately circular delaminated area of about 50 mm diameter was artificially fabricated near the center of the concrete/composite interface. This was done by applying no epoxy to that region. The GFRP plate was then pasted to the concrete block using epoxy glue. The average combined thickness of the GFRP plate and epoxy glue was found to be 4.56 mm. After the specimen was fabricated one could not see or feel the defect from outside by touching the GFRP plate because the internal delaminated area did not significantly change any dimension. The objective of the study was to detect this delamination using ultrasonic signals.

2.2. Experimental setup

A laboratory-made ultrasonic scanner [23, 25] was used for generating the ultrasonic images. A broad band Panametrics transducer was excited using a Matec 310 gated amplifier with tone-burst and short-pulse signals from the Wavetek function generator. The reflected signal was received by a Matec receiver and was digitized by a GAGE 40 MHz data acquisition board, and then the received signal was analyzed. The computer program either



Fig. 2. Tone-burst C-scan images generated by 400 kHz (top), 477 kHz (middle) and 474 kHz (bottom) signals.

computed the peak-to-peak or the average amplitude of the signal in a given time window and then plotted it in a gray scale with respect to the horizontal (x,y) position of the transducers. Voltage versus frequency or $V(f)$ curves were obtained by changing the carrier frequency of 10 cycles of the tone-burst signal and synchronous detection of the amplitude value of the received signal.

2.3. Tone-burst C-scan imaging

The first attempt was to follow a conventional pulse-echo ultrasonic C-scan imaging technique using commonly used commercially available ultrasonic transducers to detect the delamination defect. At low frequency the pulses reflected from the top surface of the composite were not well separated from those reflected from the interface. As the frequency increases the attenuation of the signal further

increases, hence a signal with a frequency larger than 5 MHz attenuates very fast and cannot penetrate deep inside the material. On the other hand, as the signal frequency decreases its resolution becomes worse because then the signal wavelength increases. Moreover, at lower frequencies (below 1 MHz) the ultrasonic wavelength becomes comparable with the thickness of the composite plate. This led us to the idea of utilizing resonance features of the composite concrete structure to distinguish the good bond from a delamination. The specimen was scanned using tone-burst signals, generated at different frequencies by the Wavetek function generator. When the 500 kHz transducer could not produce a good image showing the delamination zone either, then the excitation frequency was further reduced.

At 400 kHz excitation a faint boundary of the delamination zone could be detected (see Fig. 2a). This boundary is faint and only shows about half of the delamination boundary. Reducing the frequency further did not improve the image quality significantly. However, as the frequency was increased from 400 kHz, an improvement in the image quality was observed. At 477 kHz the delamination zone, the brighter central region in Fig. 2b, can be seen. It was observed that a small variation in the excitation frequency near 470 kHz changes the image quality significantly. For example, the image generated by the 474 kHz excitation frequency produced a much clearer image of the delamination zone (see Fig. 2c). When the frequency was increased further the image quality became worse. A number of ultrasonic scans between 100 kHz and 1 MHz were carried out and the best images were observed near 475 kHz frequency.

2.4. Interpretation of the tone-burst C-scan results

To understand why the C-scan image produced by the 475 kHz signal was much superior than that produced by the 300, 400 or 500 kHz frequency signals, the reflected amplitude voltage is plotted against the signal frequency from 250 to 1000 kHz. The three curves shown in Fig. 3 represent the reflected voltage amplitude (V) versus frequency (f) or $V(f)$ curves over the good bonded region (solid line), delaminated region (dashed line) and over the fiber composite plate only (without the concrete substrate, solid line with dot markers). It can be seen from this figure that there is a sharp dip near the 475 kHz frequency for the well-bonded composite/concrete interface; no such dips exist for the other two cases. This sharp minimum is due to the destructive interference between the front surface and the back surface reflected signals from the composite coating. Thus the composite plate acts in a similar manner to the quarter wavelength antireflection coatings of optical elements. Composite plate immersed in water and plate with free bottom surface have different (half wavelength) resonance minima which occur at different frequencies. The destructive interference frequency (the frequency

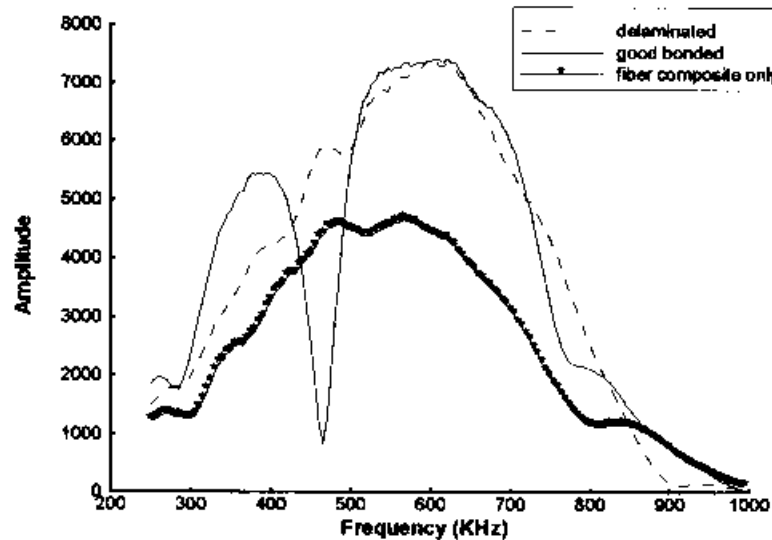


Fig. 5. $V(f)$ curves over the well-bonded region (solid line), delaminated region (dashed line) and over the fiber composite plate only (solid line with dots).

corresponding to the sharp minimum) varies from point to point because of the non-uniform distribution of glass fibers and possibly due to the non uniform glue layer. As a result, a false delamination alarm can be generated.

Although the delaminated zone can be clearly seen in Fig. 2b and c near the central region of the plate as a bright approximately circular region, there are many other bright spots in these images scattered all over the image. Does this mean that there are many spot delaminations at the interface? That is very unlikely. Those bright spots may have been created due to a change in the composite plate thickness, plate properties or glue thickness. The phase of the reflected beam changes with the plate and glue parameters as discussed above, generating a false delamination alarm. Since the dip is very sharp, a small change in the destructive interference frequency significantly alters reflected signal amplitude, hence many dark and bright spots are observed along the entire interface. It is very difficult to distinguish the bright spots caused by the delamination from those caused by the varying plate/glue properties.

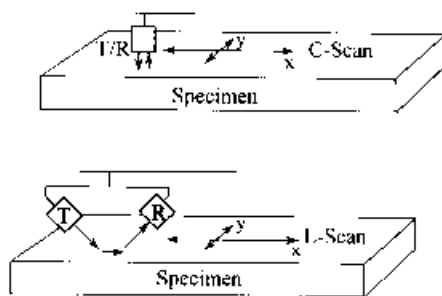


Fig. 4. Transmitter (T) and receiver (R) arrangement for conventional C-scan (top figure) and new Lamb wave scan or L-scan imaging (bottom figure).

2.5. Lamb wave scanning

Kundu et al. [23–25] have shown that Lamb waves are very effective in detecting defects inside composite plates and at the interface. To investigate the capability of the Lamb waves in detecting the concrete/composite delamination zone, the specimen was scanned by the propagating Lamb waves. In this case two identical Panametrics 500 kHz broad band transducers, one acting as a transmitter and the second one as a receiver, were used in the pitch-catch arrangement as shown in Fig. 4. Both transducers and the specimen were immersed in water. The transmitter was excited in the swept frequency tone-burst mode. The signal frequency continuously changed from 200 to 800 kHz. Transmitter and receiver were placed in the defocus position, in this position the transmitter axis and the receiver axis intersected at a point below the reflecting surface. For this orientation of the receiver the peaks in the reflection spectra were observed when leaky Lamb waves (or generalized Rayleigh waves) were generated in the specimen. This is because at the defocused position the receiver could only receive the leaky waves. Fig. 5 shows two peaks in the reflection spectrum (continuous line), one near 370 kHz and the second one near 570 kHz when the transducers are inclined at an angle of 25°. If the angle of inclination were varied the peak positions changed. If the transducers were brought closer to each other and placed in the focused position (also known as the specular reflection position) then dips were observed (dashed line) approximately at the frequency values where peaks were observed in the defocused position and vice-versa. This is because when the receiver was placed closer to the transmitter at the focus position it received direct (specular) reflected energy that was reduced when leaky waves were generated. These curves generated over the well-bonded region (Fig. 5) and the debonded region (Fig. 6) show a noticeable difference.

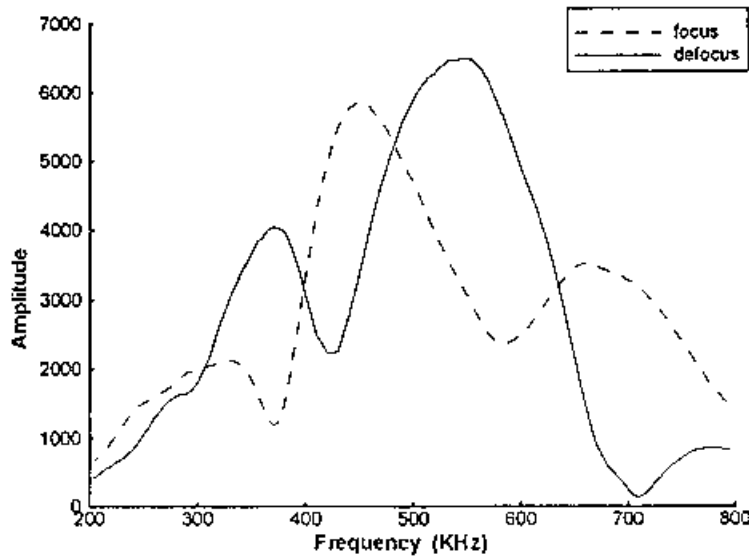


Fig. 5. $V(f)$ curves generated by propagating Lamb waves in focused (dotted line) and defocused (solid line) positions over the well bonded region of the concrete-GFRP specimen.

This implies that the Lamb wave is sensitive to the delamination defect.

One can obtain the Lamb-wave phase velocity from the transducer inclination angle using Snell's law. If the Lamb-wave phase velocity is V_L then the striking angle (θ) that would generate the leaky Lamb mode at the water-specimen interface is given by

$$\theta = \sin^{-1} \left(\frac{V_w}{V_L} \right) \quad (1)$$

where V_w is the longitudinal wave speed in water (the coupling fluid), at room temperature V_w is 1.49 km s^{-1} . From Eq. (1) one can see that a 25° angle of inclination

of the transducer corresponds to a phase velocity of 3.53 km s^{-1} . Curves similar to Figs 5 and 6 were generated for different inclinations of the transducers, varying from 10° to 27.5° . In other words, Lamb waves of different phase velocities varying from 8.58 km s^{-1} (for the 10° transducer angle) to 3.23 km s^{-1} (for the 27.5° transducer angle) were generated in the plate. Frequencies corresponding to different peaks of the received signal spectra were recorded against the Lamb-wave phase velocity. Closed and open circles in Fig. 7 show the peak positions that were experimentally obtained over the well-bonded and delaminated regions. In the frequency range of interest here (200-800 kHz) only

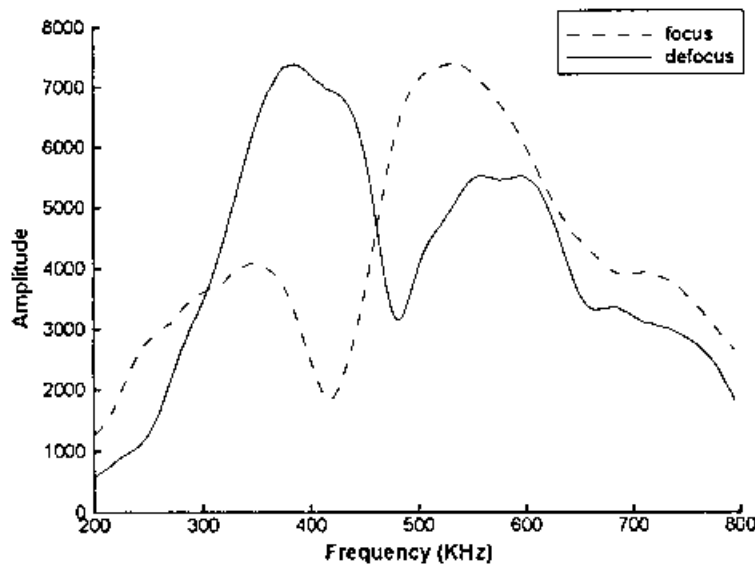


Fig. 6. $V(f)$ curves generated by propagating Lamb waves in focused (dotted line) and defocused (solid line) positions over the delaminated region of the concrete-GFRP specimen.

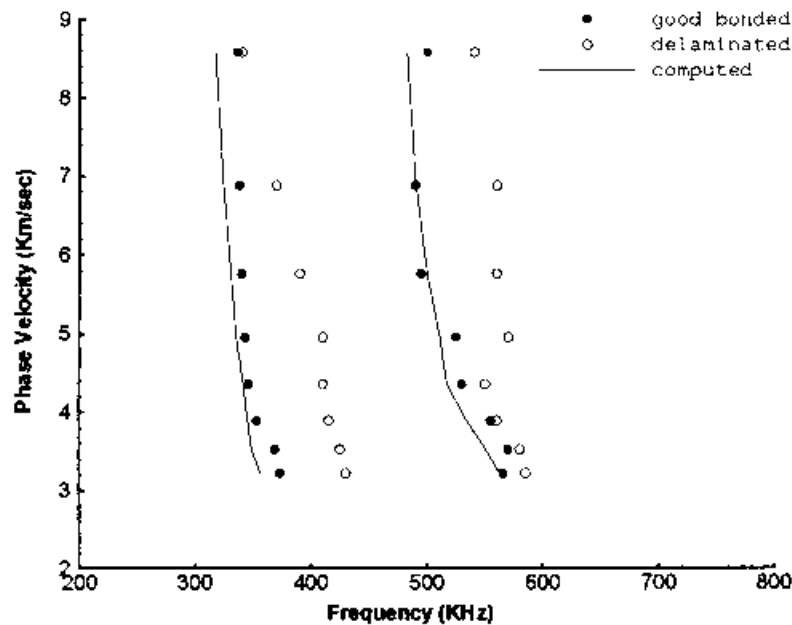


Fig. 7. Generalized Lamb/Rayleigh dispersion curves theoretically obtained (continuous line) and experimentally obtained over the well-bonded zone (solid circles) and delaminated zone (open circles).

two strong peaks were observed, whose positions shifted between 50 and 100 kHz as the transducer inclination angle changed from 10 to 27.5°.

In summary, two prominent Lamb modes were experimentally detected in our window of interest and both mode positions shifted as the transducers moved from the well bonded to the delaminated zone.

It is not easy to obtain all elastic constants of the anisotropic composite layer and compare the experimental results with the theoretical dispersion curves of the specimen. Due to the random variations of GFRP properties it was treated as a homogeneous medium at low frequencies. Ultrasonic longitudinal wave speed in GFRP was measured using a technique similar to that used by Kinra and Iyer [28, 29]. Density and elastic wave speeds in the GFRP composite layer and concrete are given in Table 1.

Reflection coefficient spectra of the composite plate (with the above material properties) sandwiched between the water half-space and the concrete half-space were computed for different incident angles between 10 and 27.5°. Sharp dips of the reflection spectra correspond to the leaky Lamb/Rayleigh wave generation frequency. Theoretical dispersion curves were computed in this manner and are plotted in Fig. 7 by a continuous line. In

spite of many approximations in the material modeling, the matching between the theoretical curves and the experimental points over the well-bonded region is quite good. Debonding shifts the dispersion curves slightly towards the right. From Fig. 7 one can see that for the lower frequency mode this shift is comparatively larger at lower phase velocity (5–3.23 km s⁻¹) or higher transducer angle (17.5–27.5°). As a result, the transducers inclined at an angle between 17.5 and 27.5° should be more effective in detecting the delamination. The 25° angle was selected for generating the L-scan image of the interface. However, any other angle between 17.5 and 27.5° would have done this job equally well.

In Fig. 5 one can clearly see that for the 25° angle of incidence the Lamb waves (or generalized Rayleigh waves) are generated near 370 and 570 kHz in the good region. On the delaminated region (Fig. 6) the strong Lamb mode is generated near 425 kHz. The specimen was scanned with this Lamb mode (incident angle = 25° and signal frequency = 425 kHz). The L-scan image of the interface is shown in Fig. 8. The delaminated zone can be clearly seen. The rest of the interface does not show any other bright spot. Clearly, the Lamb wave scanning technique is less sensitive to the variations of the glue thickness and GFRP plate properties.

Table 1
Composite layer and concrete properties

Material	Thickness (mm)	Density (g cc ⁻¹)	P-wave speed (km s ⁻¹)	S wave speed (km s ⁻¹)
GFRP	4.56	1.79	1.7	1.12
Concrete	100	6.02	4.76	2.28

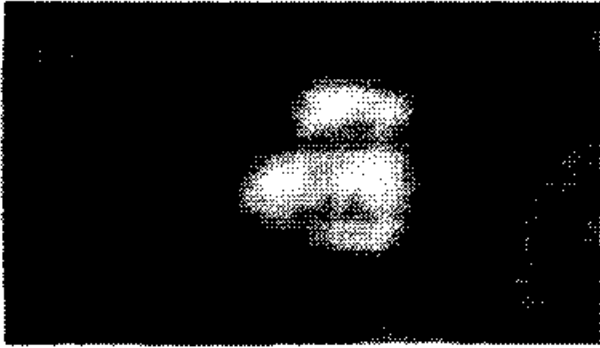


Fig. 8. Interface image generated by the Lamb wave scanning (L scan image).

2.6. Pulse-echo C-scan imaging

The specimen was also scanned by 500 kHz Panametrics transducers in the pulse-echo mode. The transducers were triggered by a JSR DPR351 pulser. The time histories over the well-bonded and delaminated zones are shown in Fig. 9. From this figure one can see that the reflected signals from the top and bottom surfaces of the composite plate are not well separated. If one plots the peak-to-peak value or the maximum signal amplitude value of this signal in a gray scale against the x,y position of the specimen then there is a good chance of completely missing the delaminated zone. This is because the reflected signal from the interface is not well separated from the front face reflection. However, by placing the receiving gate position slightly behind the front surface echo, such that it approximately coincided with the arrival time of the interface echo, one could detect the delaminated zone (top image of Fig. 10). Increasing the signal

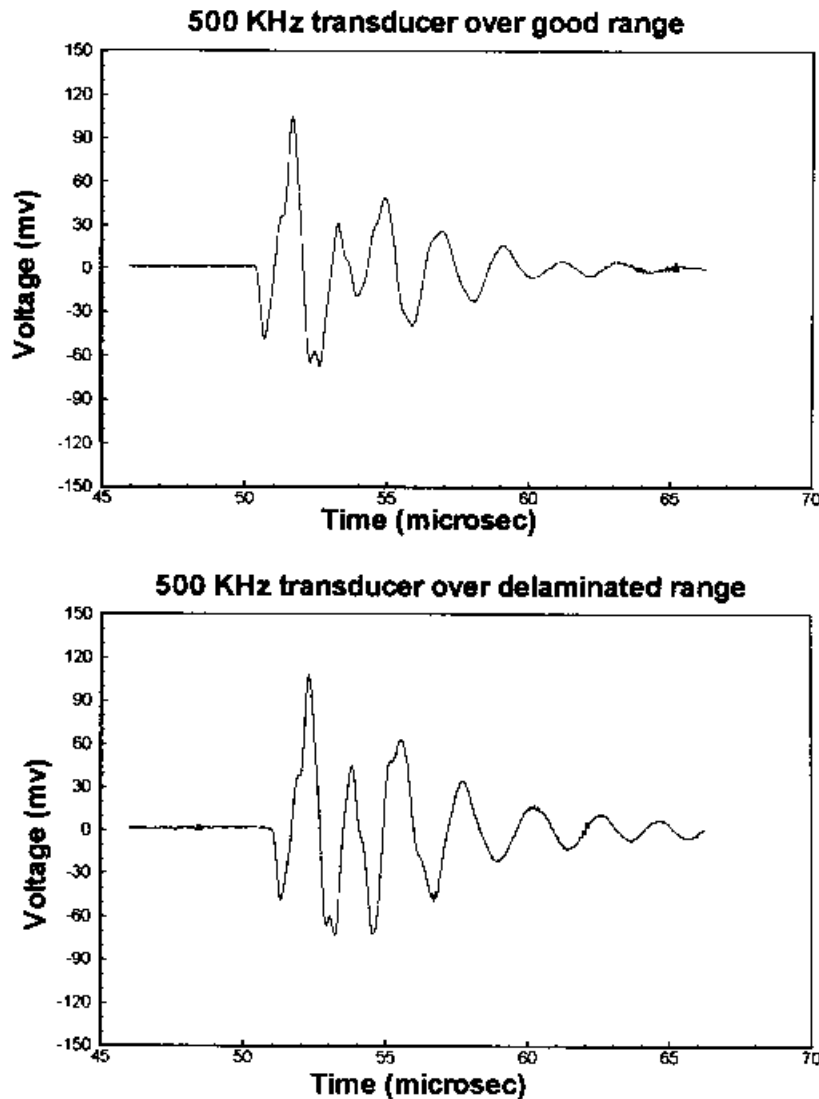


Fig. 9. Time histories generated by a 500 kHz transducer over the well-bonded zone (top) and delaminated zone (bottom).

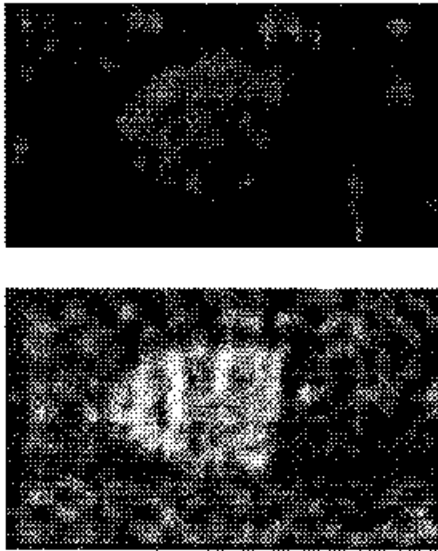


Fig. 10. Pulse-echo C-scan images of the GFRP-concrete interface generated by 500 kHz (top) and 1 MHz (bottom) transducers.

frequency to 1 MHz did not improve the quality of the image as can be seen from the bottom image of Fig. 10 which was generated by the 1 MHz transducer. One can clearly see that the qualities of both these images are worse than the L-scan image shown in Fig. 8. This is probably due to the fact that Lamb waves propagate over a finite distance along the interface before reaching the receiver. As a result, it gives the average property over that finite zone and noises in the C-scan images coming from the point-to-point property variations are eliminated in the L-scan images.

3. Concluding remarks

In this paper it is shown that the delamination at the concrete/GFRP composite interface can be detected by both Lamb wave scanning (L scan) and longitudinal wave scanning (pulse echo and tone-burst C-scan) techniques. The tone-burst C-scan technique works only at certain frequencies, corresponding to the destructive interference frequencies of the well-bonded region. The pulse-echo C-scan technique faces some difficulty because the front surface echo and the interface echo are not well separated at low frequencies and the signal attenuates very fast inside the composite layer at high frequencies. The C-scan technique is very sensitive to the glue and GFRP plate property variations, while the L-scan technique is not that sensitive to these variations. The C-scan image generated by P-waves shows similar gray levels for both delamination and glue/plate property variations. It is difficult to distinguish between the two.

The L-scan image, on the other hand, shows only the delamination zone as a bright spot. The Lamb mode used for generating the L-scan image is insensitive to the small

variations in the glue and plate properties, and as a result the image is not affected by the non-uniform plate thickness and its properties. Thus, for this application the Lamb wave scanning technique appears to be the superior technique.

Acknowledgements

This research was financially supported by NSF grants CMS9622403, CMS9523349 and EPRI Grant W08031-14.

References

- [1] Ehsani MR, Saadatmanesh H. Fiber composite plates for strengthening bridge beams. *Composite Structures* 1990;15(4):343–55.
- [2] Ehsani MR, Saadatmanesh H. Seismic retrofitting of URM walls with fiber composites. *Journal of The Masonry Society* 1996;14(2):63–72.
- [3] Ehsani MR, Saadatmanesh H. Fiber composites: an economical alternative for retrofitting earthquake damaged precast concrete walls. *Earthquake Spectra* 1997;13(2):225–41.
- [4] Chimenti DE, Nayfeh AH. Leaky Lamb waves in fibrous composite laminates. *Journal of Applied Physics* 1985;58:1531–8.
- [5] Nagy PB, Rose WR, Adler L. A single transducer broadband technique for leaky Lamb wave detection. In: Thompson DO, Chimenti DE, editors. *Review of progress in quantitative NDE*, vol. 5. New York: Plenum Press, 1986:483–90.
- [6] Nayfeh AH. Acoustic wave reflection from water-laminated composite interfaces. In: Thompson DO, Chimenti DE, editors. *Review of progress in quantitative NDE*, vol. 5. New York: Plenum Press, 1986:1119–28.
- [7] Bar-Cohen Y, Chimenti DE. Nondestructive evaluation of composites by leaky Lamb waves. In: Thompson DO, Chimenti DE, editors. *Review of progress in quantitative NDE*, vol. 5. New York: Plenum Press, 1986:1199–206.
- [8] Chimenti DE, Bar-Cohen Y. Signal analysis of leaky Lamb wave spectra for NDE of composites. In: McAvoy BR, editor. *Proceedings of 1985 IEEE Ultrasonic Symposium*. New York: IEEE, 1986:1028–31.
- [9] Martin RW, Chimenti DE. Signal processing of leaky Lamb wave data for defect imaging in composite laminates. In: Thompson DO, Chimenti DE, editors. *Review of progress in quantitative NDE*, vol. 6. New York: Plenum Press, 1987:815–24.
- [10] Mal AK, Bar-Cohen Y. Ultrasonic characterization of composite laminates. In: Mal AK, Ting TCT, editors. *Wave propagation in structural composites*, AMD vol.90. New York: ASME, 1988:1–16.
- [11] Tang B, Henneke EG. Lamb wave monitoring of axial stiffness reduction of laminated composite plates. *Materials Evaluation* 1989;47:928–34.
- [12] Bridge B, Ramli A. Nondestructive evaluation of the quality (cure) of polymer coatings on steel food cans by means of high frequency Lamb wave propagation. A preliminary study. *Journal of Materials Science* 1990;25:1794–802.
- [13] Atalar A, Keymen H, Degertekin FL. Characterization of layered materials by the Lamb wave lens. In: *IEEE Ultrasonics Symposium Proceedings*. IEEE Service Center, Piscataway, NJ, 1990:359–62.
- [14] Atalar A, Keymen H, Degertekin FL. A Lamb wave lens for acoustic microscopy. *IEEE Transactions on Ultrasonics, Ferroelectrics, and Frequency Control* 1992;39:661–7.
- [15] Chimenti DE, Martin RW. Nondestructive evaluation of composite laminates by leaky Lamb waves. *Ultrasonics* 1991;29:13–21.
- [16] Alleyne DN, Cawley P. The interaction of Lamb waves with defects. In: *IEEE Transactions on Ultrasonics, Ferroelectrics, and Frequency Control* 1992;38:1–97.
- [17] Rose JL, Ditri JF, Gallela D, Gant T. Adhesive bond inspection

- utilizing ultrasonic Lamb waves. In: *Proceedings of the 15th Annual Meeting of the Adhesion Society*, 1992:181–3.
- [18] Pilarski A, Rose JL. Lamb wave mode selection concepts for interfacial weakness analysis. *Journal of Nondestructive Evaluation* 1992;11:237–49.
- [19] Chudlis RE, Bork U. Artificial neural network processing of Lamb wave data for adhesive bond characterization. In: *Ultrasonics International '93*, Vienna, Austria. London: Butterworth-Heinemann, 1993:775–8.
- [20] Tung W, Courouble B, Royer D. Interaction of Lamb waves with a defect. In: *Ultrasonics International '93*, Vienna, Austria. London: Butterworth-Heinemann, 1993:277–80.
- [21] Courouble B, Moutle JP, Langlois B, Buckelundt B. Steel sheet testing by Lamb waves. *Revue de Metallurgie* 1994;90:835–41.
- [22] Dimitri JI, Rose JL. Excitation of guided waves in generally anisotropic layers using finite sources. *ASME Journal of Applied Mechanics* 1994;61:330–8.
- [23] Kundu T, Maslov K, Kurpur P, Matikas T, Nicolaou P. A Lamb wave scanning approach for mapping defects in [0/90] titanium matrix composites. *Ultrasonics* 1996;34:43–9.
- [24] Kundu T, Maslov KI. Material interface inspection by Lamb waves. *International Journal of Solids and Structures* 1997;34:3885–901.
- [25] Maslov KI, Kundu T. Selection of Lamb modes for detecting internal defects in laminated composites. *Ultrasonics* 1997;35:141–50.
- [26] Yang W, Kundu T. Guided waves in multilayered anisotropic plates for internal defect detection. *ASCE Journal of Engineering Mechanics* 1998;124(3):311–18.
- [27] Kundu T, Maji A, Ghosh T, Maslov KI. Detection of kissing bonds by Lamb waves. *Ultrasonics*, 1998;35:573–80.
- [28] Kinra VK, Iyer VR. Ultrasonic measurement of the thickness, phase velocity, density or attenuation of a thin viscoelastic plate. Part I: The forward problem. *Ultrasonics* 1995;33:95–109.
- [29] Kinra VK, Iyer VR. Ultrasonic measurement of the thickness, phase velocity, density or attenuation of a thin viscoelastic plate. Part II: The inverse problem. *Ultrasonics* 1995;33:111–22.